Proteolytic Fragments of Insulysin (IDE) Retain Substrate Binding but Lose Allosteric Regulation

Eun Suk Song, Clint Cady, Michael G. Fried, and Louis B. Hersh*

Department of Molecular and Cellular Biochemistry and the Center for Structural Biology, University of Kentucky, 741 South Limestone, B283 Biomedical Biological Sciences Research Building, Lexington, Kentucky 40536-0509

Received June 28, 2006; Revised Manuscript Received September 27, 2006

ABSTRACT: Treatment of an N-terminal-containing His_6-tagged insulysin (His_6-IDE) with proteinase K led to the initial cleavage of the His tag and linker region. This was followed by C-terminal cleavages resulting in intermediate fragments of ∼95 and ∼76 kDa and finally a relatively stable ∼56 kDa fragment. The ∼76 and ∼56 kDa fragments exhibited a low level of catalytic activity but retained the ability to bind the substrate with a similar affinity as the native enzyme. The kinetics of the reaction of the IDE ∼76 and ∼56 kDa proteolytic fragments with a synthetic fluorogenic substrate produced hyperbolic substrate versus velocity curves, rather than the sigmoidal curve obtained with His_6-IDE. The ∼76 and ∼56 kDa IDE proteolytic fragments were active toward the physiological peptides β-endorphin, insulin, and amyloid β peptide 1−40. Although activity was reduced by a factor of $\sim 10^3-10^4$ with these substrates, the relative activity and the cleavage sites were unchanged. Both the ∼76 and ∼56 kDa fragments retained the regulatory cationic binding site that binds ATP. Thus, the two proteinase K cleavage fragments of IDE retain the substrate- and ATP-binding sites but have low catalytic activity and lose the allosteric kinetic behavior of IDE. These data suggest a role of the C-terminal region of IDE in allosteric regulation.

Insulysin [insulin-degrading enzyme (IDE),[1] EC 3.4.22.11] is a 110 kDa zinc metalloendopeptidase first described on the basis of its ability to degrade insulin. The enzyme exhibits an oligomeric structure existing in a dimer−tetramer equilibrium, with the dimer being the predominant species (*1*). IDE cleaves insulin on both the A and B chains, with major cleavage sites on the A chain between $Leu^{13}-Tyr^{14}$ and $Tyr^{14}-Gln^{15}$. Major cleavage sites on the B chain are between Ser^9-His^{10}, $His^{10}-Leu^{11}$, $Glu^{13}-Ala^{14}$, $Try^{15}-Leu^{16}$, and $Phe^{25}-Try^{26}$ (*2*). The importance of IDE in regulating insulin levels is apparent from studies of the GK rat model of type-II diabetes mellitus. In the GK rat, naturally occurring missense mutations in the IDE gene that reduce its enzymatic activity result in an elevation in insulin levels (*3*). IDE is predominantly localized to the cytosol and peroxisomes, although secreted and plasma membrane forms have been reported (*4*). The substrate specificity of IDE is somewhat complex, with the enzyme cleaving peptides preferentially at hydrophobic and basic residues (*5*). Although it has been suggested that IDE has a preference for peptides that can form β-pleated sheet structures (*6*), *in vitro*, it effectively cleaves β-endorphin and a number of dynorphin-related peptides (*7*) that do not form such structures. Recent interest in IDE comes from the initial reports of Kurochkin and Goto (*8*) and that of McDermott and Gibson (*9*) that IDE can cleave amyloid β-peptides *in vitro*. It was found that IDE is a major amyloid β-peptide, degrading activity in a number of cell lines (*10*, *11*).

The importance of IDE in the degradation of amyloid β-peptides *in vivo* was solidified by studies with IDE-deficient mice in which the IDE gene was disrupted (*12*, *13*). Homozygous IDE-deficient mice exhibit a statistically significant increase in brain amyloid β-peptide levels, with heterozygous mice having an intermediate level. In addition, a number of genetic studies have implicated IDE as being linked to late onset Alzheimer's disease (*14*−*18*). However, this link has yet to be unequivocally established, and not all genetic studies support this linkage (*19*, *20*).

We recently reported that IDE exhibits allosteric kinetic behavior (*1*). With the synthetic substrate 2-aminobenzoyl (Abz)-GGFLRKHGQ-ethylenediamine-2,4-dinitrophenyl (EDDnp), plots of initial velocity versus [S] were sigmoidal, exhibiting a Hill coefficient greater than 2.0. In addition, when IDE substrates were tested as alternate substrate inhibitors, activation rather than inhibition was observed. Interestingly, although the peptide substrate dynorphin B-9 increased the rate of amyloid β-peptide hydrolysis by IDE, no such effect was seen with insulin as a substrate. This makes IDE a potential target for drugs that would selectively increase amyloid β-peptide clearance without affecting insulin levels.

Another form of regulation of IDE activity was first reported by Camberos et al. (*21*) in which nucleotide triphosphates were found to inhibit insulin hydrolysis by IDE. We showed that the effect of nucleotide triphosphates could be attributed to the triphosphate moiety and result from the binding of the polyanion to a cationic site on the enzyme

* To whom correspondence should be addressed: Department of Molecular and Cellular Biochemistry, University of Kentucky, 741 South Limestone, B283 Biomedical Biological Sciences Research Building, Lexington, KY 40536-0509. Telephone: (859) 323-5549. Fax: (859) 323-1727. E-mail: lhersh@uky.edu.

[1] Abbreviations: IDE, insulin-degrading enzyme; TNP-ATP, 3′(2′)-*O*-(2,4,6-trinitrophenyl)adenosine triphosphate; Abz, 2-aminobenzoyl; EDDnp, ethylenediamine-2,4-dinitrophenyl.

10.1021/bi061298u CCC: $33.50
Published on Web 11/18/2006

distinct from the active site (*22*). Although in our studies polyanions did not affect the hydrolysis of insulin or amyloid β-peptides, they increased the rate of cleavage of smaller dynorphin peptides and thus shift the specificity of the enzyme toward these smaller peptides.

To gain an insight into the structure of IDE, we have utilized limited proteolysis to determine if structural domains exist. We now report that IDE can be cleaved into a relatively stable fragment of ~56 kDa that retains substrate binding and the polyanion-binding site but not homotropic or heterotropic interactions and has significantly reduced catalytic efficiency.

MATERIALS AND METHODS

β-Endorphin was obtained from Multiple Peptide Systems through the National Institute on Drug Abuse Research Tools program. Insulin was purchased from Bachem (San Carlos CA), while amyloid β-peptide 1−40 was obtained from California Research Peptide, Inc. 3′(or 2′)-*O*-(2,4,6-trinitrophenyl)adenosine triphosphate (TNP-ATP) was obtained from Molecular Probes (Eugene, OR). Trypsin, chymotrypsin, soybean trypsin inhibitor, and diisopropylfluorophosphate were purchased from Sigma Chemical Co. (St. Louis, MO). *Staphylococcus aureus* protease V8 (proteinase V8) was purchased from Worthington Biochemical Corp. (Freehold, NJ). Proteinase K was obtained from Invitrogen. The fluorogenic substrate Abz-GGFLRKHGQ-EDDnp was synthesized as previously described (*23*).

A rat IDE cDNA, (pECE-IDE), kindly provided by Dr. Richard Roth of Stanford University (Stanford, CA), was subcloned into the baculovirus-derived vector pFastBac (Invitogen) through *Bam*HI and *Xho*I restriction sites such that a His_6-affinity tag and a linker region became fused to the N terminus of the protein. The IDE portion of the fusion protein started at methionine 42, which corresponds to the second putative start site in the coding region. The generation of recombinant baculovirus and expression of the recombinant IDE in Sf9 cells were performed according to the instructions of the manufacturer. Cells were harvested after 3 days and frozen. For the purification of recombinant IDE, a 1:10 (w/v) suspension of frozen Sf9 cells was prepared in 20 mM Tris-HCl at pH 7.4 containing 1 mM dithiothreitol. The suspension was sonicated 12 times, with each burst for 1 s, using a Branson sonifier (setting 3 at 30%), and then centrifuged at 15 000 rpm for 45 min to pellet cell debris and membranes. The supernatant containing recombinant rat IDE was loaded onto a 2 mL His-Select HC nickel-affinity gel (Sigma) that had been equilibrated with 20 mM Tris-HCl at pH 7.4 containing 1 mM dithiothreitol. After the column was washed extensively with starting buffer and then with 20 mM imidazole buffer at pH 7.4, the enzyme was eluted with 100 mM imidazole buffer at pH 7.4. The enzyme was then dialyzed against 50 mM Tris-HCl at pH 7.4 containing 20% glycerol and stored at −80 °C until use. Under these conditions, the enzyme is stable for at least 12 months. It was previously established that the hexahistidine and linker region did not affect IDE activity (*1*) and therefore were not removed in these studies.

The proteinase K digestion fragments of IDE were expressed in insect Sf9 cells as N-terminal hexahistidine fusion proteins. To accomplish this, the cDNA for rat IDE in the vector pFastBacHTb (*21*) was used as a template for polymerase chain reaction (PCR) to generate the appropriate cDNA. For the expression of the 56 kDa form of IDE (amino acids 42−534) PCR primers

5-gtgtctagagactcgacccaaccaag-3′ and
*Xba*I

5′-gtgctcgag**tca**atttgtaggaatgaatt-3′
*Xho*I stop

were used to generate an ~1.1 kb fragment, which replaced a 2.4 kb *Xba*I−*Xho*I fragment from the rat IDE cDNA in pFastBacHTb. Similarly, for the expression of the 76 kDa form of IDE (amino acids 42−705) PCR primers

5-tctgctagcaggcctgagctatgatc-3′ and
*Nhe*I

5′-gtcctcgag**tca**atcgagggcttctttta-3′
*Xho*I stop

were used to generate an ~280 bp *Nhe*I−*Xho*I fragment containing a stop codon, which was used to replace a 1.2 kb *Nhe*I−*Xho*I fragment from the rat IDE cDNA in pFastBacHTb.

We also generated two forms of His_6-IDE, in which we inserted a second TEV protease site (ENLYFQ/G) to produce the 76 and 56 kDa forms *in situ* while retaining a stoichiometric amount of the C-terminal fragment.

Proteolysis by trypsin and proteinase V8 was performed in 20 mM potassium phosphate buffer at pH 7.3. With the trypsin reaction, 1 mM $CaCl_2$ was included and adding a 10-fold molar excess of soybean trypsin inhibitor terminated the reaction. Proteolysis by proteinase V8 was terminated with 1 mM diisopropylfluorophosphate. Chymotrypsin hydrolysis was conducted in 100 mM potassium phosphate buffer at pH 7.3. The reaction was terminated by the addition of PMSF to 0.5 mM plus TLCK to 0.05 mM. The proteinase K digestion reaction was terminated by the addition of PMSF to 1 mM.

The N-terminal sequence of the stable proteinase K-generated IDE fragments was determined by automated Edman degradation performed at the Protein Structure Core at the University of Nebraska Medical Center. The molecular weights of proteinase K-generated IDE fragments were determined using a gold target with a Ciphergen PBSIIc linear MALDI−TOF mass spectrometer calibrated with peptide standards. This analysis was done at the Proteomics Core of the University of Kentucky Center on Structural Biology, which is supported in part by grant P20RR20171 from the NIH/NCRR.

IDE activity assays were conducted in reaction mixtures containing 10 μM Abz-GGFLRKHGQ-EDDnp in 50 mM Tris-HCl buffer at pH 7.4. Peptide bond cleavage resulted in an increase in fluorescence that was followed on a SpectraMax Gemini XS fluorescence plate reader at an excitation wavelength of 318 nm and an emission wavelength of 419 nm.

The rate of cleavage of insulin, β-endorphin, and amyloid β-peptide 1−40 was measured in reaction mixtures containing 10 μM peptide in 50 mM Tris-HCl buffer at pH 7.4. The rate of hydrolysis was quantified by following the decrease in the peak area of the substrate by high-performance liquid chromatography (HPLC). A C_4 reverse-phase column and a linear gradient from 0.1% trifluoroacetic

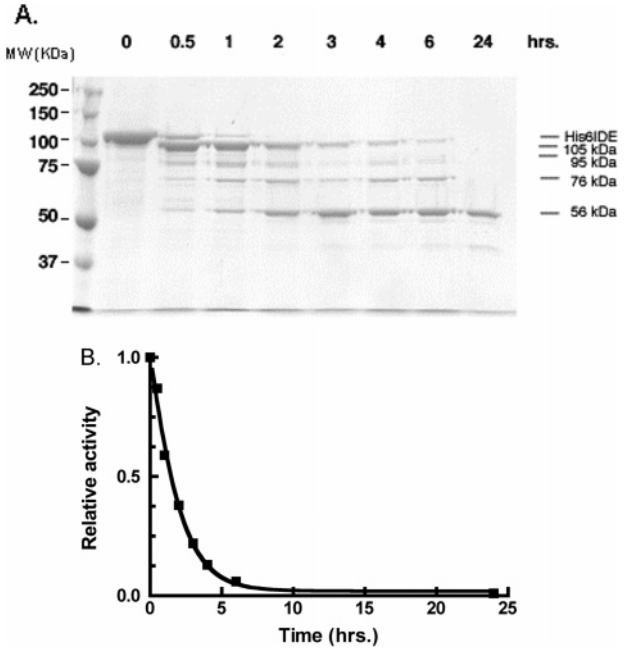

FIGURE 1: Proteinase K digestion of IDE. (A) IDE (100 μg) in 20 mM potassium phosphate buffer at pH 7.3 was treated with 0.3 μg of proteinase K in a 250 μL reaction mixture. At the time periods indicated, an aliquot was withdrawn to which was added PMSF to a final concentration of 0.8 mM to terminate digestion. This aliquot was subjected to SDS−PAGE. (B) IDE activity measurements with 10 μM Abz-GGFLRKHGQ-EDDnp as the substrate measured as a function of time of protease K digestion.

acid in 95% water/5% acetonitrile to 0.1% trifluoroacetic acid in 50% water/50% acetonitrile were employed. Peptides were followed by their absorbance at 214 nm and quantified from their peak area.

Analytical ultracentrifugation was performed at 4.0 ± 0.1 °C in a Beckman XL-A centrifuge using an AN 60 Ti rotor as previously described (*24*). Scans were obtained at 280 nm with a step size of 0.001 cm. When scans made 6 h apart were indistinguishable (~20 h), the approach to equilibrium was considered to be complete. Five scans were averaged for each sample at each rotor speed and analyzed as previously described (*24*).

The binding of TNP-ATP to IDE and its proteolytic fragments was measured in 50 mM Tris-HCl buffer at pH 7.4 using a Perkin-Elmer LS55 luminescence spectrometer.

RESULTS

In an attempt to provide insight into the domain structure of IDE, we conducted limited proteolysis experiments. Although an N-terminally His_6-tagged IDE was not cleaved by trypsin, proteinase V8, or chymotrypsin at molar ratios of up to 1:10 protease/IDE, it was cleaved by proteinase K into discrete bands. As shown in Figure 1A, over a 24 h period, proteinase K at a 1:200 molar ratio produced the sequential cleavage of the ~110 kDa His_6-IDE to produce intermediate fragments of ~105 and ~95 kDa, followed by the formation of a ~73−76 kDa fragment and finally a relatively stable ~54−57 kDa fragment. The activity declined over this time period to ~1% of the initial enzyme activity (Figure 1B). We determined the kinetics of cleavage of the synthetic substrate Abz-GGFLRKHGQ-EDDnp at 0 and 24 h of digestion and found the substrate versus velocity curves changed from sigmoidal at 0 time (Hill coefficient = 2.27) to nearly hyperbolic at 24 h (Hill coefficient = 1.38).

To identify where in the IDE molecule cleavage occurred, the 54−57 and 73−76 kDa proteinase K digestion fragments were excised from a gel and subjected to N-terminal sequencing. This procedure yielded the sequence X-N-P-A-I-Q-K for the 54−57 kDa fragment and N-N-P-A-I for the 70−73 kDa fragment. These sequences correspond to cleavage at the methionine that forms the junction between the linker region of the hexahistidine fusion protein and the N-terminal sequence of IDE (Figure 2). It should be noted that we used methionine 42 as the first amino acid for IDE because it appears that this methionine represents the major start of translation for the enzyme (*5*). Thus, both the stable 54−57 kDa and the intermediate 73−76 kDa proteinase K digestion products resulted from cleavages toward the C-terminal part of the enzyme. To obtain a more precise measure of the proteinase K cleavage sites, the IDE fragments were isolated by molecular sieve chromatography and their molecular weight was determined by mass spectrometry. A value of 56 601 Da was obtained for the smaller more stable fragment, and a value of 76 719 Da was obtained for the larger intermediate fragment; thus, we refer to these enzyme forms as IDE^{56} and IDE^{76}, respectively.

Using the mass spectral molecular weights, we generated truncated forms of IDE that corresponded to IDE^{56} and IDE^{76} (Figure 2) as hexahistidine fusion proteins in Sf9 cells using the baculovirus expression system. These were purified to homogeneity on a His-select nickel-affinity resin. The activity of these IDE fragments was verified with the fluorogenic substrate Abz-GGFLRKHGQ-EDDnp. As noted during the analysis of the protease K digestion reaction at 24 h, the sigmoidal substrate versus velocity curve seen for His_6-IDE appeared as a hyperbolic curve for IDE^{56} (Figure 3). Although not shown, a hyperbolic curve was also obtained for IDE^{76}. A summary of the kinetic data with Abz-GGFLRKHGQ-EDDnp as the substrate is given in Table 1. It can be seen from this data that both IDE^{56} and IDE^{76} retained the ability to bind the substrate with the same or increased affinity as the untreated enzyme. In contrast, both of the proteolytic fragments retained very low catalytic activity as evidenced by k_{cat} values that were ~1% of that of the wild-type enzyme. We also generated IDE^{56} (and IDE^{76}) from a full-length construct in which we inserted TEV protease sites in the appropriate positions (Figure 2). Although the IDE^{56} (and IDE^{76}) form was produced by TEV cleavage from full-length IDE, this procedure did not produce a more active enzyme nor were the allosteric properties retained.

We further tested the activity of IDE^{56} and IDE^{76} with respect to the physiological peptides β-endorphin, insulin, and amyloid β peptide 1−40. The results of this analysis are summarized in Table 2. It can be seen that in each case the residual activity is reduced by a factor of $\sim 10^3-10^4$. However, the relative activity of the two IDE truncated forms toward the physiological peptides is unchanged. Although not shown, the cleavage sites are also unchanged.

Substrate versus velocity curves for IDE^{56} (and IDE^{76}), with Hill coefficients close to 1, indicate that IDE^{56} (and IDE^{76}) do not retain the homotropic allosteric properties of His_6-IDE (or native IDE). We further tested for the presence of heterotropic activation by measuring the effect of dynor-

TEV

HHHHHHDYDIPTTENLYFQGAMNNPAIQRIEDHIVKSPELREYRGLELANGIKVLLIS

(105 kDa)

DPTTDKSSAALDVHIGSLSDPPNIPGLSHFCEHMLFLGTKKYPKENLSEHAGSSNAFT
SGEHTNYYFDVSHEHLEGALDRFAQFFLCPLFDASCKDREVNAVDSEHEKNVMNDAWR
LFQLEKATGNPKHPFSKFGTGNKYTLETRPNQEGIDVREELLKFHSTYYSSNLMAICV
LGRESLDDLTNLVVKLFSEVENKNVPLPEFPEHPFQEEHLKQLYKIVPIKDIRNLYVT
FPIPDLQQYYKSNPGHYLGHLIGHEGPGSLLSELKSKGWVNTLVGGQKEGARGFMFFI
INVDLTEEGLLHVEDIILHMFQYIQKLRAEGPQEWVFQECKDLNAVAFRFKDKERPRG
YTSKIAGKLHYYPLNGVLTAEYLLEEFRPDLIDMVLDKLRPENVRVAIVSKSFEGKTD
RTEQWYGTQYKQEAIPEDVIQKWQNADLNGKFKLPTKNEFIPTNFEILAEKDATPYPA

(56 kDa)
ENYYFQG

LIKDTAMSKLWFKQDDKFFLPKACLNFEFFSPFAYVDPLHCNMAYLYLELLKDSLNEY
AYAAELAGLSYDLQNTIYGMYLSVKGYNDKQPILLKKITEKMATFEIDKKRFEIIKEA
YMRSLNNFRAEQPHQHAMYYLRLLMTEVAWTKDELKEALDDVTLPRLKAFIPQLLSRL

(76 kDa)
ENYYFQG

HIEALLHGNITKQAALGVMQMVEDTLIEHAHTKPLLPSQLVRYREVQLPDRGWFVYQR
RNEVHNNCGIEIYYQTDMQSTSENMFLELFCQIISEPCFNTLRTKEQLGYIVFSGPRR
ANGIQGLRFIIQSEKPPHYLESRVEAFLITMEKAIEDMTEEAFQKHIQALAIRRLDKP
KKLSAECAKYWGEIISQQYNYDRDNIEVAYLKTLSKDDIIKFYKEMLAVDAPRRHKVS
VHVLAREMDSCPVVGEFPSQNDINLSEAPPLPQPEVIHNMTEFKRGLPLFPLVKPHIN
FMAAKL

FIGURE 2: Sequence of His_6-IDE showing the proteinase K cleavage sites under the sequence and the position and sequence where additional TEV cleavage sites were inserted. The arrow on the top shows where TEV cleavage occurs.

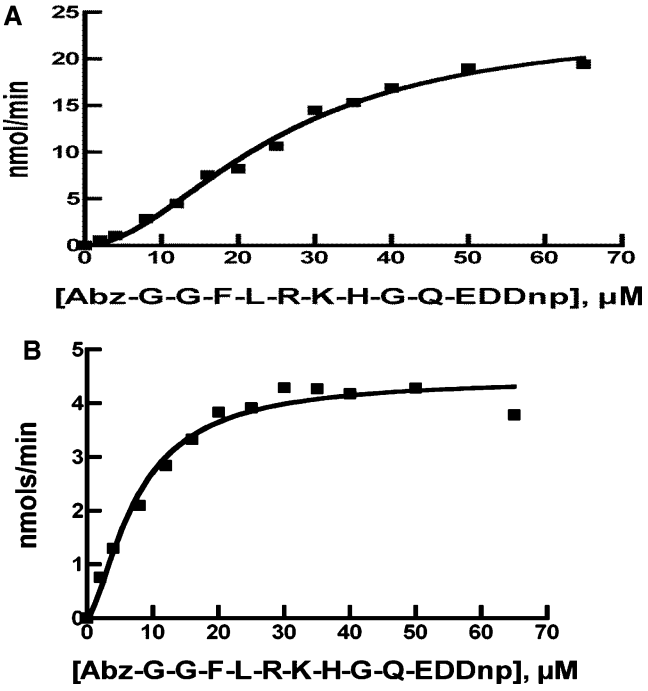

FIGURE 3: Comparison of the kinetics of wild-type IDE to IDE^{56} and IDE^{76}. Kinetics of the reaction of 0.50 μg of wild-type IDE (A) or 10 μg of the 56 kDa form of IDE, IDE^{56} (B) with Abz-GGFLRKHGQ-EDDnp in 50 mM Tris-HCl buffer at pH 7.4.

phin B-9 on the hydrolysis of the fluorogenic substrate Abz-GGFLRKHGQ-EDDnp. As previously shown with wild-type IDE, dynorphin B-9 acts as an activator of Abz-GGFLRKHGQ-EDDnp hydrolysis (*1*). Rather than produce activation, dynorphin B-9 acted as a weak inhibitor of the IDE^{56}-dependent hydrolysis of Abz-GGFLRKHGQ-EDDnp, exhibiting a K_i value of 140 μM.

Table 1: Kinetics for the Reaction of IDE and Its Proteinase K Fragments with Abz-GGFLRKHGQ-EDDnp

	K_5 or K_m (μM)	k_{cat} (min^{-1})	Hill coefficient
His_6-IDE	25.4 ± 2.4	5,590 ± 402	1.9 ± 0.2
IDE^{56}	5.9 ± 0.4	43 ± 2	1.2 ± 0.1
IDE^{76}	7.5 ± 0.9	46 ± 1	1.2 ± 0.2

Table 2: Comparison of the Reaction of Wild-Type IDE to IDE^{56} and IDE^{76} with Physiological Peptides[a]

	rate of cleavage [nmol h^{-1} (nmol of IDE)$^{-1}$]		
	β-endorphin	amyloid β peptide 1−40	insulin
His_6-IDE	18 374	4105	396
IDE^{56}	3.54	0.62	0.10
IDE^{76}	0.4	0.27	0.06
ratio of His_6-IDE/ IDE^{56}	5.2×10^3	6.6×10^3	4.0×10^3
ratio of His_6-IDE/ IDE^{76}	45.9×10^3	15.2×10^3	6.6×10^3

[a] Reactions were conducted in 0.15 mL reaction mixtures containing 50 mM Tris buffer at pH 7.4 and 10 μM peptide at 37 °C. For the reaction of wild-type IDE with β-endorphin, 25 ng of protein was used, while 50 ng of protein was used for the reactions with amyloid β peptide 1−40 and insulin. Reactions were incubated for 15−30 min. For the reaction of IDE^{56}, 10 μg of protein was used for all three peptides, with reaction times of 2−17 h. For the reaction of IDE^{76}, 20 μg of protein was used for all three peptides, with reaction times of 5−17 h. The cleavage of each peptide was followed by the disappearance of the substrate peak by HPLC. Data were quantified by the change in substrate peak area.

Because IDE exists predominantly as a dimer, we determined whether the IDE^{56} form retained this subunit structure. Sedimentation equilibrium analysis showed that IDE^{56} exists predominantly as a monomer, with some tetrameric species present. However, no dimeric IDE^{56} was detected.

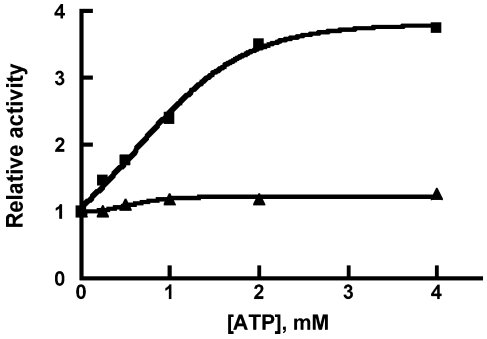

FIGURE 4: Activation of IDE^{56} and IDE^{76} by ATP. Activity was determined in 50 mM Tris-HCl buffer at pH 7.4 with 10 μM Abz-GGFLRKHGQ-EDDnp as the substrate and the indicated concentration of ATP. (■) IDE^{56} and (▲) IDE^{76}.

We have previously shown that IDE contains a cationic regulatory site distinct from the active site (*22*) that binds the triphosphate moiety of nucleotide triphosphates and free triphosphate. Binding at this site increases the rate of hydrolysis of small peptides of up to ~13 amino acids but has no effect on the rate of hydrolysis of large peptide substrates such as insulin. Using Abz-GGFLRKHGQ-EDDnp as the substrate, we tested whether the IDE^{56}- and IDE^{76}-dependent reactions were affected by ATP. As shown in Figure 4, IDE^{56} retained the ability to be activated by ATP, although to a considerably lesser extent that native IDE. The activation constant for ATP, K_A^{ATP}, was determined to be 1 mM for IDE^{56}, which can be compared to a value of 1.4 mM obtained for native IDE (*22*). ATP maximally increased the rate 6.6-fold, which is considerably less than the 40−80-fold increase seen with wild-type IDE. In contrast to the effect of ATP on IDE^{56}, we observed little if any effect of ATP on the IDE^{76}-dependent cleavage of Abz-GGFLRKHGQ-EDDnp (Figure 4).

To directly detect ATP binding, we used the fluorescent ATP analogue TNP-ATP. Binding of TNP-ATP to protein has been shown to result in an increase in its fluorescence because of a change in the environment (*25*). We first tested TNP-ATP for its ability to increase the rate of hydrolysis of Abz-GGFLRKHGQ-EDDnp with wild-type IDE and its two truncated forms. In agreement with the data using ATP, we found that 10 μM TNP-ATP increased the rate of hydrolysis of 10 μM Abz-GGFLRKHGQ-EDDnp ~125-fold (4 mM ATP increased the rate in this experiment 80-fold). With IDE^{56}, the rate was increased 3.6-fold (ATP increased the rate in this experiment 3.9-fold). However, there was no change in the IDE^{76} reaction with either ATP or TNP-ATP.

The effect of these IDE forms on TNP-ATP fluorescence is shown in Figure 5. It can be seen that TNP-ATP fluorescence is increased in the presence of 3 μM His$_6$-IDE. Although TNP fluorescence is also increased in the presence of 3 μM IDE^{56}, the magnitude of the change is considerably less. Quite surprising is the finding that the largest change in TNP-ATP fluorescence occurs in the presence of 3 μM IDE^{76}, demonstrating that the anionic binding site is in fact retained in IDE^{76}. It is also worth noting that in each case the binding of TNP-ATP shifts the fluorescence maxima to a lower wavelength, indicating that the protein-bound TNP-ATP is in a more hydrophobic environment (*26*).

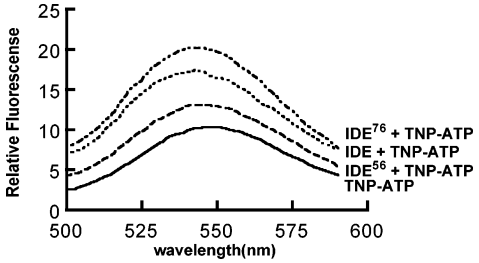

FIGURE 5: Binding of TNP-ATP to wild-type IDE and to IDE^{56} and IDE^{76}. Reaction mixtures (4 mL) contained 50 mM Tris-HCl buffer at pH 7.4, 10 μM TNP-ATP, and 3 μM wild-type IDE, IDE^{56}, or IDE^{76}. Binding of TNP-ATP was measured by the quenching of TNP-ATP fluorescence using an excitation wavelength of 403 nm and an emission wavelength of 547 nm.

DISCUSSION

Although IDE is fairly resistant to proteolysis by trypsin, chymotrypsin, and proteinase V8, it can be cleaved by proteinase K. Initially, the hexahistidine and linker region including the first methionine are cleaved leaving the N terminus of IDE, indicating that the junction between IDE and the linker region is unstructured. This is followed by C-terminal cleavages to generate 95 and 76 kDa fragments and finally another C-terminal cleavage to produce a relatively stable 56 kDa species. Because proteinase K is a broad spectrum serine protease capable of cleaving IDE in a number of places, the finding of discrete proteolytic fragments suggests that there are several unstructured regions of the enzyme within the C-terminal domains and a protease-resistant ~56 kDa core N-terminal domain.

The intermediate 76 kDa and stable 56 kDa proteinase K cleavage fragments retain a low but detectable level of catalytic activity toward the synthetic fluorogenic substrate Abz-GGFLRKHGQ-EDDnp but bind this substrate with the same or even higher affinity as native IDE. The activity of the proteinase-K-derived IDE fragments toward the physiological peptides β-endorphin, insulin, and amyloid β-peptide 1−40 is considerably lower than that toward the synthetic fluorogenic substrate. This might be interpreted to suggest that the loss of the C-terminal region may affect the ability of the enzyme to make extended binding interactions utilized in catalysis. It is likely that this results from conformational differences between the full-length enzyme and its proteolytic fragments. Thus, the proteinase K fragments fold to produce a native-like substrate-binding site but lose catalytic efficiency.

The proteinase K cleavage fragments exhibit hyperbolic substrate−velocity response curves in contrast to the sigmoidal kinetics seen with native IDE. The ability of an alternate substrate such as dynorphin B-9 to serve as an activator is lost in the 56 and 76 kDa forms, consistent with the change in kinetic properties from allosteric to classical Michaelis−Menton kinetics. In fact, dynorphin B-9 acts as a typical, although weak, alternate substrate inhibitor with the proteinase K 56 kDa cleavage fragment as would be expected for an enzyme exhibiting classical Michaelis−Menton kinetics. This would suggest that the C-terminal part of the enzyme is required for its allosteric kinetic behavior and might be responsible for either transmitting conformational changes between subunits or maintaining subunit−subunit interactions. Although native IDE exists primarily as a dimer (*1*), IDE^{56} exists predominantly as a monomer.

This suggests that the C-terminal region of IDE contains its dimerization domain and further suggest that the dimer is required for allosteric behavior.

Although the allosteric kinetic behavior of IDE is lost, the 56 and 76 kDa proteinase K cleavage fragments retain the allosteric cationic site, which binds polyanions. The 56 kDa proteinase K cleavage fragment retains the ability to bind ATP and to be activated by ATP binding, although the extent of activation appears considerably less than with native IDE. The affinity of ATP for this fragment is the same as that for wild-type IDE. Using the fluorescent ATP analogue TNP-ATP, binding was demonstrated directly. This would suggest that activation by ATP and other polyanions may involve conformational changes within IDE and does not require oligomerization. Surprisingly, the rate of substrate cleavage by the larger 76 kDa proteinase K cleavage fragment is unaffected by ATP, but this IDE form does bind ATP as shown by TNP-ATP fluorescence enhancement. Thus, we might speculate that the ~20 kDa C-terminal sequence found in the 76 kDa proteinase K cleavage fragment relative to the 56 kDa proteinase K cleavage fragment does not fold properly to permit transmission of an ATP-induced conformational change.

In summary, the 56 and 76 kDa proteinase K cleavage fragments of IDE retain an intact substrate-binding site but exhibit low catalytic activity. These IDE fragments lose the allosteric kinetic properties of IDE but retain the anion-binding site. These results suggest that the C-terminal region of IDE is needed for dimerization, a structure that is likely linked to its allosteric behavior. These smaller IDE fragments could prove useful for determining the structure of the substrate- and anion-binding sites.

While this paper was in revision, Li et al. (*27*) published a communication in which they reported that IDE expressed in *Escherichia coli* could be cleaved into ~55 and ~57 kDa fragments by trypsin. The trypsin cleavage site was near the site generating IDE[56] in this study. From the analysis of the trypsin cleavage products, Li et al. (*27*) concluded as we have that the C-terminal region of IDE is involved in oligomerization.

ACKNOWLEDGMENT

We thank Dr. Carol Beach for performing the mass spectral analysis. This work was supported in part by grants DA 02243 from the National Institute on Drug Abuse, AG 24899 from the National Institute on Aging, NS 46517 from the National Institute on Neurological Disorders and Stroke, and P20 RR02017 from the NCRR.

REFERENCES

1. Song, E. S., Juliano, M. A., Juliano, L., and Hersh, L. B. (2003) Substrate activation of insulin-degrading enzyme (insulysin). A potential target for drug development, *J. Biol. Chem. 278*, 49789−49794.
2. Duckworth, W. C. (1988) Insulin degradation: Mechanisms, products, and significance, *Endocrinol. Rev. 9*, 319−345.
3. Fakhrai-Rad, H., Nikoshkov, A., Kamel, A., Fernstrom, M., Zierath, J. R., Norgren, S., Luthman, H., and Galli, J. (2000) Insulin-degrading enzyme identified as a candidate diabetes susceptibility gene in GK rats, *Hum. Mol. Genet. 9*, 2149−2158.
4. Hersh, L. B. (2003) Peptidases, proteases and amyloid β-peptide catabolism, *Curr. Pharm. Des. 9*, 449−454.
5. Song, E. S., Mukherjee, A., Juliano, M. A., Pyrek, J. S., Goodman, J. P., Jr., Juliano, L., and Hersh, L. B. (2001) Peptidases, proteases and amyloid β-peptide catabolism, *J. Biol. Chem. 276*, 1152−1155.
6. Kurochkin, I. V. (2001) Insulin-degrading enzyme: Embarking on amyloid destruction, *Trends Biochem. Sci. 26*, 421−425.
7. Safavi, A., Miller, B. C., Cottam, L., and Hersh, L. B. (1996) Peptidases, proteases and amyloid β-peptide catabolism, *Biochemistry 35*, 14318−14325.
8. Kurochkin, I. V., and Goto, S. (1994) Alzheimer's β-amyloid peptide specifically interacts with and is degraded by insulin degrading enzyme, *FEBS Lett. 345*, 33−37.
9. McDermott, J. R., and Gibson, A. M. (1997) Degradation of Alzheimer's β-amyloid protein by human and rat brain peptidases: Involvement of insulin-degrading enzyme, *Neurochem. Res. 22*, 49−56.
10. Qiu, W. Q., Ye, Z., Kholodenko, D., Seubert, P., and Selkoe, D. J. (1997) Degradation of amyloid β-protein by a metalloprotease secreted by microglia and other neural and non-neural cells, *J. Biol. Chem. 272*, 6641−6646.
11. Qiu, W. Q., Walsh, D. M., Ye, Z., Vekrellis, K., Zhang, J., Podlisny, M., Rosner, M. R., Safavi. A., Hersh, L. B., and Selkoe, D. J. (1998) Insulin-degrading enzyme regulates extracellular levels of amyloid β-protein by degradation, *J. Biol. Chem. 273*, 32730−32738.
12. Miller, B. C., Eckman, E. A., Sambamurti, K., Dobbs, N., Chow, K. M., Eckman, C. B., Hersh, L. B., and Thiele, D. L. (2003) Amyloid-β peptide levels in brain are inversely correlated with insulysin activity levels in vivo, *Proc. Natl. Acad. Sci. U.S.A. 100*, 6221−6226.
13. Farris, W., Mansourian, S., Chang, Y., Lindsley, L., Eckman, E. A., Frosch, M. P., Eckman, C. B., Tanzi, R. E., Selkoe, D. J., and Guenette, S. (2003) Insulin-degrading enzyme regulates the levels of insulin, amyloid β-protein, and the β-amyloid precursor protein intracellular domain in vivo, *Proc. Natl. Acad. Sci. U.S.A. 100*, 4162−4167.
14. Bertram, L., Blacker, D., Mullin, K., Keeney, D., Jones, J., Basu, S., Yhu, S., McInnis, M. G., Go, R. C., Vekrellis, K., Selkoe, D. J., Saunders, A. J., and Tanzi, R. E. (2000) Evidence for genetic linkage of Alzheimer's disease to chromosome 10q, *Science 290*, 2302−2303.
15. Myers, A., Holmans, P., Marshall, H., Kwon, J., Meyer, D., Ramic, D., Shears, S., Booth, J., DeVrieze, F. W., Crook, R., Hamshere, M., Abraham, R., Tunstall, N., Rice, F., Carty, S., Lillystone, S., Kehoe, P., Rudrasingham, V., Jones, L., Lovestone, S., Perez-Tur, J., Williams, J., Owen, M. J., Hardy, J., and Goate, A. M. (2000) Susceptibility locus for Alzheimer's disease on chromosome 10, *Science 290*, 2304−2305.
16. Ertekin-Taner, N., Graff-Radford, N., Younkin, L. H., Eckman, C., Baker, M., Adamson, J., Ronald, J., Blangero, J., Hutton, M., and Younkin, S. G. (2000) Linkage of plasma Aβ42 to a quantitative locus on chromosome 10 in late-onset Alzheimer's disease pedigrees, *Science 290*, 2303−2304.
17. Li, Y. J., Scott, W. K., Hedges, D. J., Zhang, F., Gaskell, P. C., Nance, M. A., Watts, R. L., Hubble. J. P., Koller, W. C., Pahwa, R., Stern, M. B., Hiner, B. C., Jankovic, J., Allen, F. A., Jr., Goetz, C. G., Mastaglia, F., Stajich, J. M., Gibson, R. A., Middleton, L. T., Saunders, A. M., Scott, B. L., Small, G. W., Nicodemus, K. K., Reed, A. D., Schmechel, D. E., Welsh-Bohmer. K. A., Conneally, P. M., Roses, A. D., Gilbert, J. R., Vance, J. M., Haines, J. L., and Pericak-Vance, M. A. (2002) Age at onset in two common neurodegenerative diseases is genetically controlled, *Am. J. Hum. Genet. 70*, 985−993.
18. Ait-Ghezala, G., Abdullah, L., Crescentini, R., Crawford, F., Town, T., Singh, S., Richards, D., Duara, R., and Mullan, M. (2002) Confirmation of association between D10S583 and Alzheimer's disease in a case−control sample, *Neurosci. Lett. 325*, 87−90.
19. Abraham, R., Myers, A., Wavrant-DeVrieze, F., Hamshere, M. L., Thomas, H. V., Marshall, H., Compton, D., Spurlock, G., Turic, D., Hoogendoorn, B., Kwon, J. M., Petersen, R. C., Tangalos, E., Norton, J., Morris, J. C., Bullock, R., Liolitsa, D., Lovestone, S., Hardy, J., Goate, A., O'Donovan, M., Williams, J., Owen, M. J., and Jones, L. (2001) Substantial linkage disequilibrium across the insulin-degrading enzyme locus but no association with late-onset Alzheimer's disease, *Hum. Genet. 109*, 646−652.
20. Boussaha, M., Hannequin, D., Verpillat, P., Brice, A., Frebourg, T., and Campion, D. (2002) Polymorphisms of insulin degrading

enzyme gene are not associated with Alzheimer's disease, *Neurosci. Lett. 329*, 121−123.
21. Camberos, M. C., Perez, A. A., Udrisar, D. P., Wanderley, M. I., and Cresto, J. C. (2001) ATP inhibits insulin-degrading enzyme activity, *Exp. Biol. Med. 226*, 334−341.
22. Song, E. S., Juliano, M. A., Juliano, L., Fried, M. G., Wagner, S. L., and Hersh, L. B. (2004) ATP effects on insulin-degrading enzyme are mediated primarily through its triphosphate moiety, *J. Biol. Chem. 279*, 54216−54220.
23. Csuhai, E., Juliano, M. A., Pyrek, J. S., Harms, A. C., Juliano, L., and Hersh, L. B. (1999) New fluorogenic substrates for *N*-arginine dibasic convertase, *Anal. Biochem. 269*, 149−154.
24. Song, E. S., Daily, A., Fried, M. G., Juliano, M. A., Juliano, L., and Hersh, L. B. (2005) Mutation of active site residues of insulin-degrading enzyme alters allosteric interactions, *J. Biol. Chem. 280*, 17701−17706.
25. Hiratsuka, T. (2003) Fluorescent and colored trinitrophenylated analogs of ATP and GTP, *Eur. J. Biochem. 270*, 3479−3485.
26. Huang, S. G., Weisshart, K., and Fanning, E. (1998) Characterization of the nucleotide binding properties of SV40 T antigen using fluorescent 3′(2′)-*O*-(2,4,6-trinitrophenyl)adenine nucleotide analogues, *Biochemistry 37*, 15336−15344.
27. Li, P., Kuo, W. L., Yousef, M., Rosner, M. R., and Tang, W. J. (2006) The C-terminal domain of human insulin degrading enzyme is required for dimerization and substrate recognition, *Biochem. Biophys. Res. Commun. 343*, 1032−1037.

BI061298U